A review on the use of activating flux in gas tungsten arc welding towards obtaining high productivity

Samarendra Acharya[1], Santanu Das[2*]

[1,2]Kalyani Government Engineering College, Kalyani, West Bengal, India
[1]Global Institute of Management and Technology, Nadia, West Bengal, India

KEYWORDS

Welding,
GTAW,
TIG Welding,
ATIG Welding,
Activating Flux,
Penetration,
Productivity.

ABSTRACT

This paper mainly focuses on the review of activated flux TIG welding, more commonly known as ATIG, or activated TIG, welding. Tungsten inert gas welding is an imperative process since quality of the welds produced is high. In this process, productivity is usually low and to overcome this limitation, ATIG welding is often used to achieve improved productivity through enhanced penetration. Application of a thin coating of activating flux is made onto the faying surface prior to ATIG welding. By employing ATIG welding, it may be possible to weld 8-10 mm thick stainless steel plates as compared to 2-3 mm in conventional TIG welding. As activating flux, some oxides, chlorides, fluorides, etc. are used with acetone, or alcohol, etc. as the solvent. In ATIG welding, input parameters are chosen such as welding current, welding speed, percentage of activating fluxes, etc. to achieve weld bead with deep penetration and consequently high aspect ratio.

1. Introduction

Gas Tungsten Arc Welding (GTAW) or Tungsten Inert Gas (TIG) welding is performed by creating an arc between a non-consumable tungsten electrode and the work piece to be welded. It is used in those cases where accurate welding as well as precision welding is essentially desired (Korkman & Meran, 2020; Wu et al., 1997; Chen et al., 1990; Katoh, 1990). However, due to lack of productivity and low depth of penetration, research works were undertaken since long to improve depth of penetration as well as productivity. Increased productivity in ATIG welding signifies greater depth of penetration, i.e. 8-10 mm in stainless steel instead of 2-3 mm in conventional TIG welding. Increased productivity can be derived by reducing welding time through enhanced penetration and requiring less number of welding passes.

Activated Flux TIG welding, known as ATIG welding, was first utilized in the late 1950s by the EO Paton Institute of Electric Welding. ATIG welding fetches enhanced penetration. As 2 to 3 mm depth of penetration could be achieved by TIG welding with single pass, but 10 to 12 mm depth of penetration could be achieved with single pass by using activating flux in ATIG welding. So, more than 300% increment could be achieved by this process (Saha & Das, 2018). Active fluxes are those fluxes that will cause a substantial change in the weld metal chemistry when welding voltage and consequently, the amount of flux fused is changed. Activated Tungsten Inert Gas (A-TIG) welding is one variant of conventional TIG welding process where a thin layer of appropriate activating flux is applied on the base plates prior to welding. Practically, application of the activating flux on the base plates prior to welding is the only difference between conventional TIG and ATIG welding; however, the results in terms of weld bead characteristics vary to a large extent as well as weld penetration. Commonly used activating fluxes for ATIG welding are chromium oxide (Cr_2O_3), magnesium carbonate ($MgCO_3$), magnesium oxide (MgO), manganese dioxide (MnO_2), calcium oxide (CaO), aluminium oxide (Al_2O_3), zirconium dioxide (ZrO_2) etc. as shown in Fig.1 (Singh & Khanna, 2021).

Powdered fluxes of particle size 30-60 µm are mixed with appropriate solvent (mostly acetone) to prepare a semi-solid mixture. This paste is then applied on faying surfaces and surrounding areas of the base plates (Fig.2) (Zhang et al., 2011). Application of activating flux offers several benefits like increased depth of penetration due to reversal of Marangoni Effect, reduced weld

*Corresponding author E-mail: sdas.me@gmail.com

https://doi.org/10.58368/MTT.22.7-8.2023.12-28

bead width, constricted arc, narrow HAZ, less distortion, etc. Among the fluxes, SiO_2, TiO_2, MoO_3, CuO, Co_3O_4, MoS_2 are effective as single component flux. As binary fluxes SiO_2 + TiO_2 mixed in the ratio of 90:10 or 80:40 and MoO_3+ SiO_2 mixed in the ratio of 4:1, Fe_2O_3+ Cr_2O_3 mixed in the ratio 89:11 and as ternary flux SiO_2+ TiO_2+ Cr_2O_3 produced remarkable effect in respect of depth of penetration.

2. Mechanism for Deep Penetration

2.1. Reversed marangoni effect

The Marangoni effect (also called the Gibbs–Marangoni effect) is the mass transfer within two fluids due to a gradient of the surface tension (Figure 3). In the case of temperature dependence, this phenomenon may be called thermo-capillary convection (or Bénard-Marangoni convection).

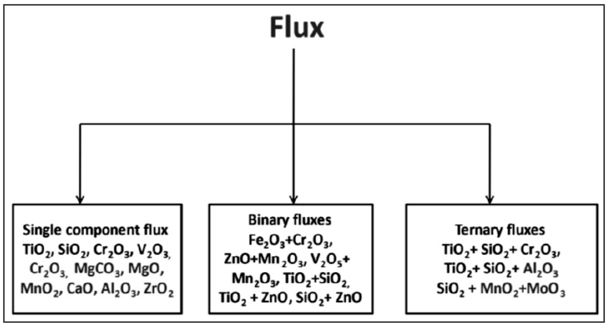

Fig. 1. Different oxide fluxes used in activated flux TIG welding (Singh & Khanna, 2021).

Thermal coefficient of surface tension (TCST) is responsible to change the direction of movement of molten pool of weld material. If the surface tension gradient is negative, the cooler part will be the outer region of the molten pool as compared to the central part. So, more surface tension will be generated at the outer region compared to that at the central part. As a result, direction of flow of the molten pool will be in the outward direction creating a wide and shallow weld pool. However, due to the presence of surface active elements such as oxygen, sulphur and selenium present in an active flux, as proposed by Heiple and Roper (Shahroudi & Halvaei, 2019), temperature dependence of surface tension becomes positive from negative and flow of direction of molten weld pool will be towards central region, and then flows down starting from outward region. As a result of this, high depth of penetration can be achieved. This is known as reversed Marangoni effect (Xu et al., 2007; Bhattacharya, 2015; Lin & Yang, 2020).

2.2. Arc constriction effect

Arc constriction can also be the possible reason behind high penetration (Howse & Lucas, 2000; Kumar et al., 2009; Lin & Wu, 2012).

Arc Constriction is due to insulating properties of flux. Metallic oxides are mostly used as fluxes and they are electrical insulators, and hence, surfaces covered by such fluxes have higher electrical resistance. This reduces size of arc spot and increases penetration.

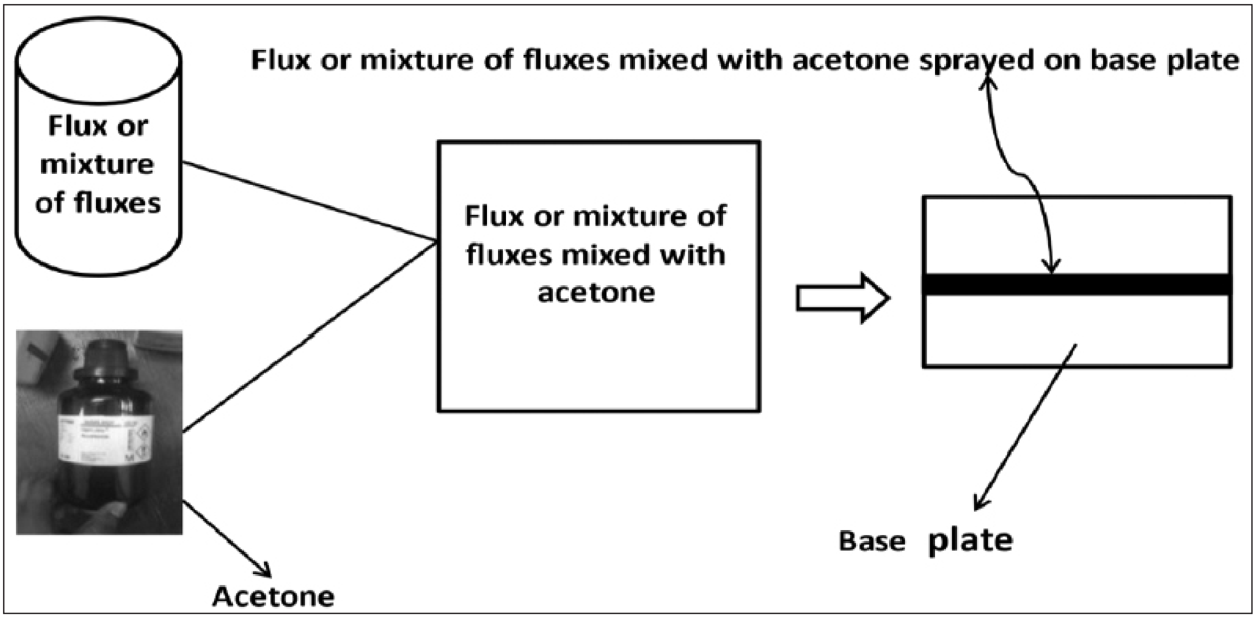

Fig. 2. Application of flux for ATIG welding process.

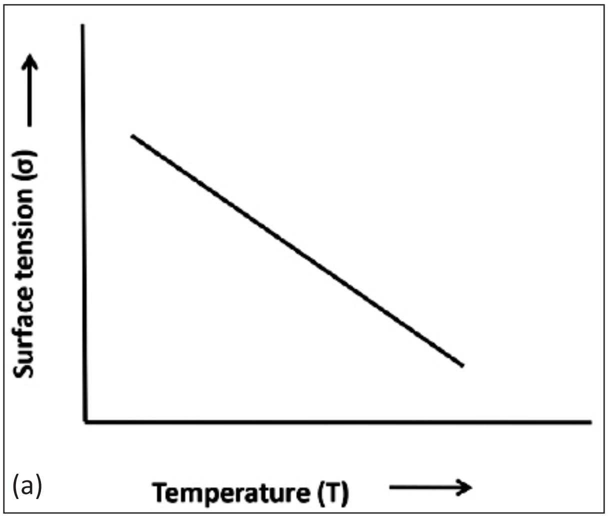

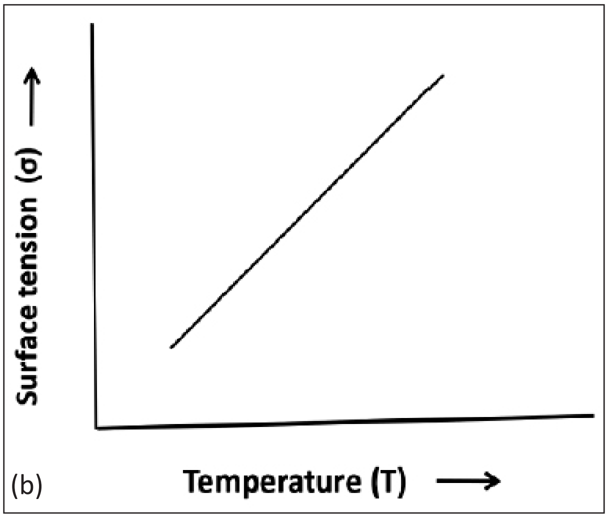

Fig. 3. Typical variation of surface tension with change in temperature in (a) TIG and (b) ATIG welding.

3. Theories Regarding High Penetration in ATIG Welding Process

3.1. Theory of simonik in 1976

This theory tells Shahroudi and Halvaei (2019) that oxide and fluorine atoms existing in the activating flux create remarkable entity to drag free electrons at the corner edge of the plasma of the arc. It is stated that ions formed in this way acquire substantially lower ability to move than free electrons. So, at the central portion of the arc, density of arc increases enormously due to higher moveability of electrons.

3.2. Theory of savitskii and Leskov in 1980

This theory implies Shahroudi and Halvaei (2019) that the activating fluxes possess the ability to decrease surface tension as well as lower the anodic spot and consequently result in deeper penetration.

3.3. Theory of Heiple and Roper in 1982

According to this theory as reported by Shahroudi and Halvaei (2019), deeper penetration can be achieved with the help of reversed Marangoni effect. When the surface tension gradient becomes negative, the flow of molten pool occurs from centre to the edge of the molten pool. It is known as Marangoni effect. On the other hand, due to the presence of active fluxes, surface tension gradient changes its value from negative to positive and as a result, the direction of molten pool starts from surface end towards the centre of the molten pool. It is known as Reversed Marangoni effect and it is considered to be the main reason behind achieving high penetration during ATIG welding.

3.4. Theory of Lowke, Tanaka and Ushio in 2005

According to this theory, the activating flux is responsible to cause an insulating surface all-around the arc region and consequently, the arc causes deeper penetration (Shahroudi & Halvaei, 2019).

4. Predictor Factors of ATIG Welding

Many determinant factors are responsible Sandor & Dobranszky (2007) to cause deep penetration as well as productivity as stated below:

1. Root gap: The joint gap i.e. root gap is a major factor in case of butt joint. Basically, higher currents (i.e., 550-650 A) for a root face of 8-10 mm is required for a zero root gap butt joint. In this case, welding on both sides is mandatory for achieving favourable depth of penetration. Here, heat input is also to be checked. For circular seam welding, zero root gap is required.
2. Welded joint: If the root gap is more than a prescribed limit, then inclusions may occur. In case of ATIG welding, zero root gap is to be maintained, otherwise it will create a problem from the industrial point of view.
3. Thickness as well as quantity of flux to be applied: Thickness of paste should be around 20-25 µm (except for TiO_2, the paste thickness should be around 40 µm). The quantity of flux should be around 0.1 to 0.15 gm/m according to international literature on ATIG welding.

4. Method of applying flux: Human errors may arise while applying flux to generate uniform desired thickness of flux cover. However, human errors need to be eliminated or reduced substantially by suitable ways and means.
5. Selection of tungsten electrode: In ATIG welding, lower amperage is required as compared to higher amperage in TIG welding. Although high penetration is achieved using low amperage in ATIG welding, but visibly high heat load gets developed which ultimately leads to faster disbursement of electrode. So, it is necessary for monitoring high heat input.

5. Types of Welding Current Used for ATIG Welding

There are generally three types of welding current used in TIG welding, such as DCSP, DCRP and AC (Mohan, 2014; Afolalu et al., 2019). These are discussed in the following:

DCSP (Direct Current Straight Polarity) or DCEN (Direct Current Electrode Negative): In it, tungsten electrode is connected to the negative terminal and work piece is connected to the positive terminal. It is used in consideration of high depth of penetration and shallow weld bead.

DCRP (Direct Current Reverse Polarity) or DCEP (Direct Current Electrode Positive): In it, tungsten electrode is connected to the positive terminal and work piece is connected to the negative terminal. It is mainly used for light weight material with low amperage.

AC (Alternating Current): It is mainly used for aluminium and magnesium materials. One part of the square wave form is used for cleaning action and the other part for welding with deep penetration.

6. Enhancement of Penetration in Flux Assisted TIG Welding of Various Types of Materials

6.1 Flux assisted TIG welding of aluminium and its alloys

Yong et al. (2007) reported the effect of multi-component flux AF 305 on aluminium alloy. They used different polarities DCSP, DCRP and AC to show the effects of flux on weld penetration. It was shown that AC polarity created better weld penetration as compared to other direct current polarities and resulted deep penetration more than 3 times that of conventional TIG welding. It was also stated that when AF 305 was used as activating flux, some portions of welding slag got separately distributed on weldment and constriction of arc pool happened. In another work conducted by Reddy et al. (1998), they explained the effect of pulse frequency during TIG welding with respect to micro structure, hardness and tensile strength of AA8090 type Al-Li alloy treated with AA5356 filler. They showed that pulsed current during TIG welding resulted in finer equiaxed grain structure as compared to coarse columnar grain structure in continuous current TIG welding process. It was also revealed that grain refinement was associated with increase of hardness, UTS and ductility. They also stated that within the optimum frequency range of 6 to 8 Hz, grain refinement was the highest.

An experiment was performed by Zhou and Huang (2014) to show the effect of mono component fluxes such as TiO_2, SiO_2, Cr_2O_3, V_2O_5 and halide CaF_2 on 5052 aluminium alloy. They showed that TiO_2 and SiO_2 took major role causing greater depth of penetration as well as narrow heat affected zone. Another research work conducted by Li et al. (2017) explained the effects of AlF_3, LiF, KF-AlF_3, and K_2SiF_6 on 2219 aluminium alloy by using DCEN welding and VP (variable polarity) TIG welding and comparison were made among these processes. They stated that DCEN ATIG welding showed no porosity in the weld zone instead of several micro and macro porosity observed during VP TIG welding. Coarse grain structure was observed in VPTIG welding due to large current as compared to reduced current in DCEN ATIG welding.

Al-SiC composite was welded by Singh et al. (2017) using pulsed current ATIG welding giving improved mechanical properties as compared to ATIG, PCTIG and conventional TIG welding. In the same year, DCEN ATIG welding was reported by Li and Zou (2017) to be more effective with respect to avoid porosity and achieving deep penetration as compared to convetional TIG welding. They used the fluxes such as AlF_3, LiF, KF-AlF_3, and K_2SiF_6 and 2219 alluminium alloy was considered as base metal. Hui and Jiashengi (2017) carried out an experiment to show that the active agent, AlF_3- 75% LiF had better effect during DCEN active flux TIG welding on 2219 aluminium alloy. This active flux was reported to be much responsible to remove surface oxide and welding pores to improve the weld surface quality. A report on the influence of welding parameters on mechanical properties such as tensile strength, hardness, etc. was made by Varshney & Kumar (2021) during TIG welding and activated flux TIG welding. Better microstructure analysis of welded joint of aluminium AA5456 was reported. Better microstructure properties and mechanical properties such as hardness, etc. were evaluated by taking welding current as the varying parameter. Here welding electrode of grade 4047 was used for more content of silicon for increasing fluidity during welding operation.

6.2 Research works based on magnesium alloy

The effect of $CdCl_2$ as the activating flux was reported by Liu et al. (2006) during ATIG welding on AZ31B magnesium alloy. To improve mechanical properties by adding ceramic particles with activating flux were also experimented by (Liu & Su, 2008). During their experiment, they used 60% TiO_2 + 40% SiC by using base metal AZ31B. Another research work showed by Li et al. (2012) the effect of single component fluxes (TiO_2, Cr_2O_3 or SiO_2) during A-TIG welding in AC mode by using base metal AZ31B magnesium alloy.

Shen et al. (2013) showed the effect of SiC mixed with TiO_2 as a flux during experimentation with ATIG welding. They used hot extruded AZ 31 magnesium alloy plates of sizes 100 mm x 50 mm x 6 mm. When the amount of TiO_2 was increased up to 70%, the depth of penetration was found to be increased and consequently D/W ratio was also increased. Authors also concluded that nano sized SiC particles produced more micro hardness value as compared to micro sized SiC particles. It was also revealed that when the amount of nano sized particles reached 40%, the UTS value of fusion zone of the welded portion achieved maximum value.

Another work carried out by Shen et al. (2014) showed the effect of current during their experimentation with activated flux TIG welding. They used AZ 31 magnesium alloy plates of sizes 100 mm × 50 mm × 6 mm as base metal. They selected TiO_2 as flux with particle size of 120 nm. They concluded that with the increase of current, D/W ratio increased and at the same time width of welded seam was also found to have increased. They also stated that when current value reached too high, D/W ratio decreased and deterioration of surface of base metal occurred. An experiment was carried out by Zhou et al. (2017) to show the effects of Cr_2O_3 flux and ageing treatment on microstructure and mechanical properties of TIG welded AZ31 magnesium alloy joints. It was reported that Cr_2O_3 flux exhibited higher D/W ratio of the welded joint as compared to conventional TIG welding. The average micro hardness of fusion zone of the ATIG welded joint was greatly improved by ageing treatment. It was also reported that the ageing treatment improved ultimate tensile strength and elongation of the ATIG welded joint.

The effect of fluorine free and fluorine content coating on AZ31 magnesium alloy was observed by Fu et al. (2019). They took the sample size as 30mm x20mm x 5mm. The main constituent of coating in the fluorine-free electrolyte was MgO and MgO + MgF_2 as coating component in fluorine electrolyte. On the contrary, when KF content in the electrolyte was increased, porosity of the coating surface decreased. Some other group Guiqing et al. (2020) experimented on AZ91 magnesium alloy plates with dimensions 100 mm x 100 mm x 5 mm. They reported the influence of magnetic field on microstructure and mechanical properties of AZ91 magnesium alloy welded joint in ATIG welding. The results obtained were compared with or without the use of magnetic field. When the parameters of magnetic field and activated flux matched, larger depth of penetration and smaller form factor were obtained. Welding efficiency was improved at the same time. It was also stated that at the activated flux amount of 3 gm cm^{-2}, optimal values of mechanical properties of welded joint such as tensile strength of 385 MPa, elongation of 13.3%, and hardness of 67HV were obtained. Although the combined action of magnetic field and activated flux had no significant effect on phase composition of weld seam, but the crystallization nucleation of molten pool was changed, finer grain size was formed, and formation of twins was attained.

A different team Tanaka et al. (2000) carried out experiments taking base plate as SUS 304 measuring 150 mm x 50 mm x 6 mm with helium as shielding gas and pure TiO_2 as activated flux. It was reported that D/W ratio of welds with flux was much higher as compared to welds without flux which were independent of current. It was shown that surface tension got abruptly lowered with the increase in coating density of flux. The change of surface tension was stated to be the same as change of depth of penetration.

It was concluded that in GTAW process with flux, metal plasma was localised at the centre of the weld pool as compared to wider metal plasma in the weld pool occurred in GTAW process without flux. There was a constricted anode root in case of flux assisted GTAW as compared to diffused anode root in case of conventional GTAW process. The anode root can found to be related to temperature distribution on the weld pool surface. Multiplication effect of Lorentz force and reversed Marangoni effect were found to be fully responsible to cause the inward flow of the weld pool.

6.3 Research works based on stainless steel and dissimilar metals

A method was applied by Kumar et al. (2009) to improve welding efficiency and mechanical properties of the welded joint. It was revealed that transverse section of weld pool section of ATIG welds showed inward flow lines even in low sulphur content stainless steel. It was concluded that productivity obtained with ATIG welding was higher compared to conventional TIG welding. Kuo et al. (2011) made an extensive study between TIG welding and ATIG welding and concluded that aspect ratio, i.e. depth/width ratio, had been more with flux than that without flux. They used G3131 mild steel and SUS 316 L stainless steel as dissimilar alloys. As oxide fluxes, they used SiO_2, Fe_2O_3, Cr_2O_3, and CaO. TIG welding without flux produced clean and smooth weld surface whereas TIG welding with flux produced residual slag on the surface. On consideration of weld morphology, TIG welding without flux produced wider and shallower weld bead, whereas TIG welding with fluxes like SiO_2, Fe_2O_3 and Cr_2O_3 produced narrow weld bead and deep penetration. CaO flux had no significant effect on weld morphology. Authors also concluded that TIG welding without flux produced lower angular distortion in the weldment whereas TIG welding with flux produced higher angular distortion.

Lin & Wu (2012) experimented on Inconel 718 alloy with TIG welding with single component flux such as SiO_2, NiO, MoS_2 and MoO_3 and mixed component fluxes such as 50% SiO_2+50% MoO_3 and 50% SiO_2+ 50% NiO, the later produced better depth of penetration as well as D/W ratio of the weldment. In another work, Song et al. (2018) concluded that a wide scope for researchers existed to use Mg/steel dissimilar welding. The main feature of this hybrid welding is their large difference in melting point temperature. Other team of researchers such as Vasantharaj and Vasudevan (2012); Manivannana et al. (2020); Sharma and Dwivedi (2021); Afolalu et al. (2021); Chandrasekar et al. (2020); Vinothkumar et al. (2020); Silva et al. (2020) applied a flux during stainless steel tube welding. It was beneficial in respect of deep penetration and productivity. It was also applied during bead-on-plate welding on mild steel and ferritic stainless steel. It was reported to be helpful in respect of elimination of edge preparation, reduced distortion and increase of productivity.

The effect of self developed flux on P91 graded steel was reported by Arivazhagan & Vasudevan (2013) in another work. They explained the effect of self developed flux on mechanical properties and evaluated microstructure of p91 graded stainless steel. Untempered martensitic microstructure was observed in the welded joint. Microinclusion content was low and low volume fraction of delta ferrite was found in the weldment. Due to presence of untempered martensite, impact toughness was low. Impact toughness was also increased due to increasing tempering time at 760^0C. An experiment was executed by Cai et al. (2016) with the help of TIG welding by applying boron oxide flux on base metal BS700MC super steel. Boron oxide played a vital role to increase the depth of penetration by constricting the arc and reversing Marangoni convection in the weld pool. It was stated that when base metal was pasted with boron oxide as flux material, the microstructure of the heat affected zone generated a large amount of acicular structure causing the weld joint low temperature impact toughness. It was also concluded that boron oxide could significantly reduce the current required for penetration. As a result, softening degree of heat affected zone reduced due to reduced heat input.

Ruckrt et al. (2014) carried out an experiment on plain carbon and stainless steels, titanium and aluminum by applying fluxes. They chose silica for plain carbon steel, stainless steel and aluminium. On the other hand, they chose fluorides based fluxes for titanium. A flux coating of 15 mm width was applied around the joint area. It was reported that in ATIG welds, depression in the weld pool was observed at higher current and it was hardly visible in TIG welding at higher current. They reported a confined arc was created on the surface of base metal due to the presence of flux coating on the surface. Due to presence of flux coating, high power density of arc was produced to cause deep penetration.

Venkatesan et al. (2014) performed experiment on AISI 409 ferritic stainless steel plates with the use of TiO_2, SiO_2 and Cr_20_3 as fluxes. The ATIG process was reported to be better in respect of depth of penetration and increment of productivity than conventional TIG welding. It was concluded that 86% increase of depth of penetration was achieved with the help of the fluxes used. It was also stated that SiO_2 flux in mixed condition with other fluxes produced greater depth of penetration as compared to 100% SiO_2 flux. It was also observed that residual slag was formed on the surface during ATIG welding which should be removed. Consequently, clean weld was formed on the surface during TIG welding. Another group Zou et al. (2014) reported an experiment on ATIG welding of SUS329J4L duplex stainless steel by the use of double shielding gas with the use of different oxygen content levels. The outer layer was controlled by controlling the oxygen levels and the inner layer remained filled with pure argon to suppress the oxidation of the electrode. Due to dissolution of oxygen in the weld metal, large depth of penetration was observed. On the other hand, microstructure of the weld metal was completely changed due to dissolution of oxygen.

An attempt to show the effect of two different fluxes, SiO_2 and Fe_2O_3 on AISI 430 ferritic stainless steel was made by Ramkumar et al. (2015) during ATIG welding. It was revealed that SiO_2 and Fe_2O_3 fluxes could be successfully employed to achieve desired depth of penetration by using single pass welding instead of double pass welding without flux. The existence of ferrite, Wid-manstatten austenite and low carbon martensite clusters were observed by examining microstructure analysis of fusion zone of base plate. Low carbon martensite was responsible to increase the hardness of the fusion zone as compared to the parent metal. Joint strength efficiency obtained with Fe_2O_3 weldment was found to be 87.5% whereas joint strength obtained was more than parent metal for autogeneous TIG welding with or without the use of SiO_2 flux. Depth of penetration could be increased (Ramkumar et al., 2015) by the application of SiO_2 flux on AISI 904L super austenite stainless steel. Trials were made on bead-on-plate welding to show the effect of heat input and current on depth of penetration. Optimal values of process parameters were validated by employing the experimental investigations to ascertain the structure-property relationship of activated flux TIG welding.

Experiments were carried out by Vora & Badheka (2015) with base metal as ferritic/martensitic (RAFM) steel. Different oxide fluxes Al_2O_3, Co_3O_4, CuO, HgO, MoO_3, and NiO were used by considering bead-on-plate welding maintaining constant values of process parameters. Size of specimen was 75mm x 25mm x 6mm and pure acetone was taken as solvent. It was concluded that spatter was found on weld bead surface when Co_3O_4 was used whereas in case of CuO flux, spatter was found on the lower side, although Co_3O_4 and CuO are responsible to cause deep penetration. However, successfully full penetration was achieved with Co_3O_4 and CuO fluxes. Highest D/W ratio was achieved as 0.95 by using the flux Co_3O_4. Micro hardness values and microstructure remained unchanged during TIG and ATIG weldment. The HAZ as well as weld region was noticed to have a combination of fine grained and coarse grained structure. Moghaddam & Kolahan (2020a) showed the effect of SiO_2 nano–powder flux on base plate AISI 316L stainless steel. The size of the specimen was 100mm x 50mm x 10mm and 99.99% pure argon was used as shielding gas. Ethanol was used as a solvent. In this study, formulation had been done by regression modelling which was characterised by depth of penetration and welding bead width as a function of input parameters such as welding current, welding speed and root gap. Based on ANOVA results, the best fitted model had been selected and Taguchi optimization technique was used to optimize the best suited model and the experimental results.

Patel et al. (2021) exprimented on Chromium manganese austenitic stainless steel of 5 mm thick using SiO_2 and TiO_2 as flux. It was reported that reversed Marangoni and arc constriction effect resulted in higher productivity as well as lower consumable cost. It was stated that tensile strength and hardness value of ATIG welded specimen was more as compared to conventional TIG welded specimen. In another experiment conducted by Vora et al. (2021), they reported the effect of TiO_2 flux on SA 516 Gr. 70 carbon steel material of specimen thickness 6 mm. In this work, the input parameters were selected as welding current, arc length and torch travel speed. The responses namely heat input, heat affected zone, D/w ratio and depth of penetration were optimised by the combinations of RSM (Response Surface Methodology) and HTS (Hough Transform Statistics) algorithms.

Chandrasekar et al. (2020) observed fusion welding to be the best suited method for industrial application. ATIG process was associated with less bead width and high depth of penetration with less heat input. Proper flux material was selected for individual material to get the desired benefit from ATIG welding. The effect of oxide fluxes on 316 stainless steel was reported (Roy et al., 2017) in some other work. It was reported that different ratios of flux mixtures such as SiO_2 and TiO_2 mixed in the ratios of 1:1, 4:1 and 1:4 were used to get the desired depth of penetration. SiO_2 had more pronounced effect on depth of penetration as compared to TiO_2. More depth of penetration was achieved when SiO_2 and TiO_2 mixed in the ratio of 4:1 and 1:1 were used. Full penetration of 5 mm was achieved with the valid condition at 120A current, 17.9 V voltage and 140 Hz frequency when SiO_2 and TiO_2 were mixed in the ratio of 1:1. Weld bead appearance was reduced to some extent in ATIG weldment due to addition of flux mixtures. An experiment was performed by (Saha & Das, 2018). They applied fluxes, TiO_2, Cr_2O_3 and Fe_2O_3, on 316L stainless steel base plate of thickness 6 mm during their experimentation with ACATIG welding. Welding was done both on bead-on-plate welding and butt joining. Different weld features such as weld bead width, depth of penetration, reinforcement, reinforcement form factor (RRF), penetration shape factor (PSF) against different heat input values were discussed and compared. It was revealed that TiO_2 & Fe_2O_3 resulted in high depth of penetration as well as narrow weld width. On the other hand, Cr_2O_3 flux was ineffective in respect of causing depth of penetration as well as to reduce weld bead width.

Dhandha & Badheka (2015) reported on the effect of 6 different activating fluxes such as CaO, Fe_2O_3, TiO_2, ZnO, MnO_2 and Cr_2O_3 on P91 graded stainless steel of thickness 6 mm. Bead- on-plate welding was done under 100% pure argon shielding gas to avoid the effect of root gap and edge preparation. Surface appearance was satisfactory after using activating flux on the base plate. It was stated that heat input increased with the use of activating flux and each oxide was found to possess capability of reducing bead width as well as increasing depth of penetration depending on physical-chemical properties of the oxides.

Leconte et al. (2007) carried out experiments to show the effects of various fluorides such as BaF_2, CaF_2, Na_3AlF_6, MgF_6 on 304L stainless steel. They also used different fluoride mixtures during their experimentation. The size of the specimen was 200 mm x 50mm x 4 mm. In this work, the combined effect of arc physics and chemistry of base metal were investigated. It was revealed that the electrical arc energy density and ionic radius of the element were responsible to cause the activating effect of the fluorides. They stated that fluoride fluxes were not capable of producing any effect on base metal. A global or a local arc temperature increased which was largely dependent on fluorides that could be observed by optical spectrometry of the arc. In another experiment conducted by Bodkhe & Dolas (2018), they showed that the effect of the activating flux SiO_2 on 304L stainless steel was very significant in consideration of depth of penetration. They took current, welding speed and arc gap as input variables whereas depth of penetration as response. Response surface methodology with central composite design was taken as design of experiment. From ANOVA table, it was clear that the three process parameters i.e. current, weld speed and arc gap were most significant and current was stated to be the top most significant input criteria. By taking the random values of welding current, weld speed and arc gap, regression equation was established for predicting the response.

Afolalu et al. (2020) showed that FeO nano particle flux powder could be prepared from the waste organic material coconut shell, by reduction process. The chemical reaction followed such as coconut shell + $FeSO_4.H_2O \rightarrow FeO + C$. It was revealed that the nano particles of flux powder was successfully applied to improve properties of the welded joint in case of activated flux TIG welding and metal inert gas welding process. Singh et al. (2017) reviewed to state that in TIG welding wider weld pool and shallow depth of penetration of weld was achieved. So, to overcome these difficulties of TIG welding, the author proposed to use ATIG welding, FBTIG welding and pulsed current TIG welding. It was stated that pulsed current TIG welding was better in respect of increased depth of penetration, narrow weld pool and better weld quality.

A report on bead-on-plate welding on 306 grade stainless steel with similar grade filler was made by (Saha & Das, 2019) using TiO_2, Cr_2O_3 and Fe_2O_3 as flux material. Both AC and DCEN polarity was used on 6 mm thick plates and compared with the required benefits achieved in comparison with TIG welding. TiO_2 flux required lower heat input with DCEN polarity compared to AC polarity. When Cr_2O_3 was used with the same heat input and DCEN polarity and AC polarity, no appreciable increment in depth of penetration could be obtained. Using Fe_2O_3 flux, lower heat input was evolved compared to TiO_2 flux. TiO_2 flux produced 6.98 mm depth of penetration compared 5.64 mm produced by Fe_2O_3. Cr_2O_3 produced the same depth of penetration as produced by conventional TIG welding with the same heat input. Another work Saha and Das (2020) showed the effect of impact of different mono component fluxes on 306 stainless steel by using DCEN polarity during ATIG welding. Slag formation was observed on the weld bead when TiO_2 and Fe_2O_3 were used as flux. Cr_2O_3 flux produced little slag on weld bead. TiO_2 and Fe_2O_3 showed potential capability of increasing depth of penetration and narrow weld bead width. On the contrary, Cr_2O_3 flux played no role of improving depth of penetration and shortening weld bead width.

Fujii et al. (2008) showed the effect of double shielding gas [He-O_2 and He-CO_2] on SUS 304 stainless steel to have greater depth of penetration. It was revealed that under welding speed of 0.75 mm/s, welding current of 160 A and electrode gap of 1 mm under the He–0.4%O_2 shielding, the depth/width ratio could be increased remarkably. In another work reported by Babbar et al. (2019), multi-component TiO_2-SiO_2-Al_2O_3 hybrid Flux was used on SS304 to have deep penetration of 8.283 mm with current of 110 A, speed of 82 mm/min and flow rate of 14 l/mm. In the research work carried out by Bhattacharya (2015), he showed that the reversed Marangoni convection and Lorentz force both might be responsible to drive the molten pool from periphery towards the centre of the weld pool. The workpiece material used was 304 stainless steel of size 105 mm x 95 mm x 6 mm and different fluxes such as SiO_2, TiO_2, CrO_3 and MoS_2 were used in doing the experiment. Due to the presence of oxygen in the activating fluxes, arc constriction effect was observed which was responsible to increase heat density and consequently temperature of the weld pool resulting in depper weld pool.

Pandya et al. (2020) showed reversed Marangoni effect and arc constriction effect to be responsible to cause higher heat input and consequently, larger depth of penetration. Activated fluxes having more electronegativity create more constricted arc column resulting in deeper penetration. Different concentrations of surface active elements played a remarkable role to change surface tension gradient and ultimately depth of penetration. It was also revealed that smaller sized particles of activated fluxes showed higher depth of penetration than larger sized particles. An increase of current showed higher depth of penetration, and increase in weld speed as well as increase in arc length were found to cause reduced depth of penetration.

Magudeeswaran et al. (2014) experimented on duplex stainless steel as base plate (ASTM/ UNS:S32205) of size 100 mm x 150 mm x 6 mm and Ador ATIG Flux -1 which was a typical banned activating flux used to enhance the depth of penetration and narrow weld bead. Butt joint was made during ATIG welding. They took electrode gap, torch travel speed, current and voltage as input parameters and weld bead width, depth of penetration and aspect ratio were taken as responses. In this experimental work, optimisation was done by Taguchi's orthogonal array (OA) as experimental design method and statistical tools such as analysis of variance (ANOVA) and pooled ANOVA techniques. There was no solidification cracking in the weldment when ATIG welding was done on DSS weld joint. In an experimental work conducted by Li et al. (2018), they showed the influence of TiO_2, NaCl and CaF_2 activating fluxes on 5 mm stainless steel plate. Pulsed TIG welding with 2% thoriated tungsten electrode and DCEN polarity was used in the experiment. Average surface tension of the molten weld pool was measured with the help of a new surface tension measurement system. Absolute value of surface tension gradient decreased when TiO_2 flux was used. It was revealed that due to increase of coating density, surface tension gradient also increased and approached a maximum value. Further increase of coating density resulted in a decrease of surface tension and ultimately reached to zero. They reported that NaCl and CaF_2 reduced the average value of surface tension but created little effects on surface tension gradient.

Niagai (2021) repoted the effects of activating fluxes Cr_2O_3, TiO_2, SiO_2, Fe_2O_3, NaF and AlF_3 on unalloyed (carbon) steel S235JR+N as well as fine-grained steel grades P265GH (for pressure vessels) and S355J2+N. It was concluded that TiO_2 and SiO_2 played a vital role to increase the depth of penetration independent of grades and types of steel. Other oxides and fluorides were dependant on types and grades of steel. As for example, the sodium and the aluminium fluorides decreased depth of penetration on weld of austenitic stainless steel and depth of penetration was increased by the use of the above fluorides in case of fine grained steel. LAFM and SS 316 LN dissimilar weld joint of 6 mm thickness was made by (Patel et al., 2019). They used five different fluxes such as TiO_2, Fe_2O_3, CuO, Co_3O_4 and HgO to make a comparative study with TIG welding. Experiments were performed on bead-on-plate welding under the same welding conditions and parameters. Surface appearance was inferior in ATIG weldment compared with TIG welded joint. Too much spatter was found in ATIG weldment with Co_3O_4 flux. They also stated that higher D/W ratio was exhibited by Co_3O_4 and TiO_2 flux. Arc constriction effect and reversed Marangony effect were effective in case of TiO_2 and Co_3O_4. But in case of other fluxes, arc constriction effect was totally absent. A course grained LAFM HAZ changed to fine grained LAFM base metal. But in case of 316 L HAZ and 316L base metal, there was no change of microstructure.

Saha et al. (2021) carried out an experiment on base plate AISI 316L stainless steel of 10 m thick austenitic stainless steel. They took Cr_2O_3, Fe_2O_3 and SiO_2 as single component fluxes with DCEN polarity by forehand welding technique under varying welding current. Squre edged butt joint was prepared for ATIG welding. Current in the range of 120A -150A were used for comparing effect of these fluxes on base plate. It was reported that depth of penetration was increased with the increase of current and consequently high heat input, but excessively high current produced high heat input which was responsible to cause wider weld bead and HAZ, higher rate of distortion and breakage of the refractory cap at the top of the torch. Reinfocemement dropped gradually with the increase of current while filler deposition rate remained unchanged. Among the three fluxes, Fe_2O_3 caused 134-140% more depth of penetration compared to conventional TIG welding, and SiO_2 flux caused remarlably well depth of penetration i.e. 9.15 mm or 160% to 174% increase of depth of penetration in comparison with conventional TIG welding. Highest value of RFF and lowest value of PSF were observed in case of SiO_2 flux. Cr_2O_3 based flux produced more micro hardness value compared to Fe_2O_3, and SiO_2 based ATIG welding. HAZ and weld bead width were lower in case of Fe_2O_3, and SiO_2 based ATIG weldment compared to Cr_2O_3 based ATIG welding. Saving of time was significant in case of Fe_2O_3 and SiO_2 based ATIG welding.

Sahu et al. (2021) experimened on stainless steel 316L and Alloy 800 of size 6 mm thickness. They used two different components of fluxes such as Flux A– 35% TiO_2, 40% SiO_2, 15% NiO, 10% CuO and Flux B– 35% TiO_2, 40% SiO_2, 15% ZnO, 10% MoO_3. It was reported that flux B produced higher depth of penetration compared to flux A component. Visual defects were absent in macrograph and microstructures of the weld locations. Acharya and Das (2020) reviewed on the effects of various activating fluxes on different types of materials such as alluminium alloy, magnesium alloy, stainless steel and dissimilar metals. It was stated that three kinds of polarity of current were used in ATIG welding such as DCSP (direct current straight polarity) or DCEN (direct current electrode negative), DCRP (direct current reverse polarity) or DCEP (direct current electrode positive) and AC (alternating current). In view of increase of depth of penetration as well as productivity benefiets, ATIG welding can be highly recommended to industries. The Analytical hierarchy process (AHP) was successfully applied by Acharya and Das (2022) for finding out the optimised input parameters and responses with the experimental values conducted by (Magudeeswaran et al., 2014). It was stated that 9 experimental runs were conducted by taking the input parameters such as heat input, weld speed and electrode gap and depth of penetration as response. As flux, AdorAeTIG and as base metal, UNSS32205 duplex stainless steel were used during experimentation. The AHP, a multicriteria decision making tool was used to explore the optimal depth of penetration and productivity benefiets in ATIG welding. Reversed Marangoni effect and arc constriction effect could be the main mechanism causing deep penetration in ATIG welding.

7. Different simulations / algorithms adopted for optimisation / prediction in ATIG welding

To attain deep penetration during ATIG welding and to determine sinificance of each process variable to achieve deep penetration, ANOVA was carried out by Magudeeswaran et al. (2014); Moghaddam and Kolahan (2020) and others during their experimentation on duplex stainless steel welds. Back propagation neural network (BPNN) with corresponding hidden layer numbers with the number of neurons/nodes was applied by Moghaddam and Kolahan (2021) to find the suitable model to get the output or response. On the other hand, opmisation was done by utilising

SA (simulated annealing) and PSO (particle swarm optimization) algorithms to find maximum depth of penetration, favourable aspect ratio and minimum weld bead width. Confirmation tests taking experimental values were carried out to validate predicted values. The optimal experimental values were in close proximity with the predicted values. Different works carried out by Chaudhary et al. (2015) showed how the AHP could successfully be implemented for prediction purposes. In a particular work carried out by Capraz et al. (2015), they stated that AHP-TOPSIS hybrid model could effectively be applied for selection of the best supplier fulfililing different criteria to suit green supply chain management.

8. Conclusion and Future Scope of Work

From the present review, the following may be concluded:

- Some of the mixture of fluxes such as SiO_2, Al_2O_3 and TiO_2, not only took the responsibility of increasing the depth of penetration, but also initiated to enhance surface appearance of weldment with a single pass and thus, increased productivity could be obtaind.
- Among various active fluxes used by the researchers, SiO_2 and TiO_2 are quite common. Use of activated flux could increase penetration of weldment while welding stainless steel, mild steel, nickel based alloys, magnesium based alloys, P91 steel, etc. although a specific activated flux for a particular application not yet explored.
- An effective range of flux quantities for different active fluxes are required for a particular application to enhance penetration. Flux coating thickness on the joint surface is an essential factor in ATIG welding. It was revealed that with increment of flux densty, depth of penetration increased considerably. It was reported that about 200 mg/m flux quantity is sufficient in ATIG welding but any amout more than that may produce flux residue.
- Increase of penetration could not be obtained effectively by the use of Al_2O_3 flux. Al_2O_3 crystal structure creates a cover over the metal below and creates a shielding atmosphere to protect from atmospheric contamination and thus limiting depth of penetration could be achieved via diffusion of oxygen through aluminium oxide.
- Oxygen content in the weld pool generally was found to take major role in increasing depth of penetration due to reversal of surface tension gradient from negative to positive over a certain range of thickness of material from 70-300 ppm for different materials. Enhancement of weld penetration may not be possible if the oxygen content in the weld is too high or too low.
- Stability and particle size of the flux can have a remarkable effect when the flux is allowed to decompose under the arc. The arc is unable to decompose a too-stable or too-large sized particles and so, they will produce no significant effect on the activated flux TIG welding.
- Reversed Marangoni and arc constriction mechanisms are responsible to cause deep penetration in the weld pool. Activated fluxes having more electronegativity create more constriction of the arc column and produce deep penetration.
- Addition of H_2, He, O_2 and N_2 in argon as shielding gas can cause a hike of depth of penetration by increase of heat input during ATIG welding. Effects of hydrogen addition with helium was observed. Firstly, arc voltage is increased due to high thermal conductivity of hydrogen. Secondly, due to high thermal conductivity of hydrogen at the dissociation temperature, arc shape and colour is altered. Due to addition of hydrogen, bead geometry is also changed. Depth of penetration is increased while the bead width remains unaltered and consequently, aspect ratio is increased. Furthermore, increase of heat input due to increase of weld cross sectional area. Due to addition of oxygen with argon shielding gas, some changes is observed in liquid weld pool characteristics. When the oxygen content is increased beyond the critical value of 70 ppm, the liquid weld pool characteristics is changed from wide shallow type to deep narrow one followed by reversed Marangoni flow from outer direction to inward flow direction of the liquid molten weld pool. When 10% nitrogen is added with argon shielding gas, sudden changes in mechanical properties is observed. Tensile strength of sample can be raised by 15% as well as its fatigue life. As helium has a high thermal conductivity and heat carrying capacity than argon, high heat input is created when helium is mixed with argon and as a result deeper penetration is observed in the workpiece. This is particularly

useful for thicker material and when deeper weld pool is desired.

- In case of various metals, higher hardness and tensile strength can be achieved in fusion zone during ATIG welding than conventional TIG welding. Microstructure of the ATIG weldment shows that due to formation of columnar and equiaxed grain structure in the fusion zone of ATIG weldment, tensile strength and hardness are more than convensional TIG weldment.
- To increase toughness and to minimise the effect caused by residual stress in ATIG welding, post-weld heat treatment (PWHT) is required. At the centre of the welded joint of ATIG weldnent, compressed residual stresses arise due to sudden contraction and expansion of the liquid weld pool. This residual stress can be minimised by post weld heat treatment. To achieve a desirable weldment, post weld heatment is requied as it is shown that if the postweld heat treatment is done above AC1 temperature, fresh marensite is formed and as a result, lower toughness and higher hardness is observed. If post weld heat treatment (PWHT) is done 20^0 below the AC1 temperature, highest toughness and lowest hardness are obtained at the heat affected zone of ATIG weldment.
- Degrading of weld appearance may occur due to high amount of slag on weld surface by the entrapped oxide flux. FB-TIG (flux bound tungsten inert gas) welding can largely eliminate this drawback and takes advantages over ATIG welding. In flux bound tungsten inert gas (FB-TIG) welding, flux is not pasted on faying surface and all around it; but, it is applied on the upper surface of base metal keeping small space after root gap. So during welding flux does not adhere just below electric arc.
- In this field, lot of works can be done by considering flux composition, heat input, size of particle, coating thickness and arc length to get desired depth of penetration and mechanical properties.
- Different simulations/ algorithms can be applied to optimize the process. Simulation-based optimisation methods which are most commonly used, are Statistical ranking and selection methods (R/S), Heuristic methods, Stochastic approximation, Derivative-free optimization methods. Dynamic programming and neuro-dynamic programming. Particle swarm optimization (PSO), Artificial Neural Network (ANN), Analytical Heirarchy Process (AHP), etc. are also used.
- There is also a greater scope for the researcher as little work is done on some materials such as AISI 321, Inconel X-750, aluminium alloys, etc.
- In this work, an overview is made to report effects of various process parameters such as welding current, welding speed, heat input, electrode diameter, etc. on responses like tensile strength, hardness, depth of penetration, etc. by a suitable optimisation technique.
- Ressearchers have the scope to compute continuous temperature distribution towards the weldment and to minimise width of heat affected zone (HAZ) to get high penetration, and hence, productivity during A-TIG welding.

References

Acharya, S., & Das, S. (2020). Effect of activating flux in gas tungsten arc welding. *Weld Fab Tech Times, 4,* 12-21.

Acharya, S., & Das, S. (2022). Achieving favourabe depth of penetration and productivity of ATIG welds utilising the AHP. *Indian Science Cruiser, 36,* 17-23.

Afolalu, S. A., Ikumapayi, O. M., Emetere, M. E., & Ongbali, S. O. (2021). Investigation of mechanical properties and characterization of a joint using nano flux powder for A-TIG welding. *Materials Today: Proceedings, 44,* 2879-2883.

Afolalu, S. A., Samuel, O. D., & Ikumapayi, O. M. (2020). Development and characterization of nano- flux welding powder from calcined coconut shell ash admixture with FeO particles. *Journal of Materials Research and Technology, 9,* 9232-9241.

Afolalu, S. A., Soetan, S. B., Ongbali, S. O., Abioye, A. A., & Oni, A. S. (2019). Impact of activated flux tungsten inert gas (A-TIG) welding on a weld joint of a metal - review. *Ist International Conference on Sustainable Infrastructural Development, IOP Conference Series: Materials Science and Engineering*, 640.

Ahmad, A., & Alam, S. (2019). Parametric optimization of TIG welding using response surface methodology. *Materials Today: Proceedings, 18,* 3071-3079.

Ahmadi, E., Ebrahimi, A. R., & Khosroshahi, R. A. (2013). Welding of 304L stainless steel with activated tungsten inert gas process (A-TIG). *International Journal of ISSI, 10,* 27-33.

Arivazhagan, B., & Vasudevan, M. (2013). A study of microstructure and mechanical properties of grade 91 steel in FBTIG weld joint. *Journal of Materials Engineering and Performance, 22,* 3708-3716.

Babbar, A., Kumar, A., & Gupta, D. (2019). Enhancement of activated tungsten inert gas (A-TIG) welding using multi-component TiO_2-SiO_2-Al_2O_3 hybrid flux. *Measurement, 148,* 106912/1-16.

Bodkhe, S. C., & Dolas, D. R. (2018). Optimization of activated tungsten inert gas welding of 304L austenitic stainless steel. *Procedia Manufacturing, 20,* 277-282.

Balos, S., Dramicanin, M., Janjatovic, P., Kulundzic, N., Zabunov, V., Pillic, B., & Kiob, C. D. (2020). Influence of metallic oxide nanoparticles on the mechanical properties of an A-TIG welded 304l austenitic stainless steel. *Materials, 13,* 1-11.

Bhattacharya, A. (2015). Revisiting arc, metal flow behavior in flux activated tungsten inert gas welding. *Materials and Manufacturing Processes,* 1-22.

Bose, S., & Das, S. (2021). Experimental investigation on bead-on-plate welding and cladding using pulsed GTAW process. *Indian Welding Journal, 54,* 64-76.

Cai, Y., Luo, Z., Huang, Z., & Zeng, Y. (2016). Influence of oxides on microstructure and mechanical properties of high strength steel weld joint. *High temperature Materials and Processes, 35,* 1047-1053.

Capraz, O., Meran, C., Worner, W. A., & Gungor, A. (2015). Using AHP and TOPSIS to evaluate welding processes for manufacturing plain carbon stainless steel storage tank. *Archives of Materials Science and Engineering, 75,* 157-162.

Chandrasekar, G., Kannan, R., Prabakaran, M. P., & Ganesamoorthy, R. (2020). Effect of activating flux (Metal Oxide) on the weld bead nomenclature of tungsten inert gas welding process – a review. *IOP Conf. Series: Materials Science and Engineering, 988,* 012084.

Chaudhary, R., Jat, M. L., Nandal, D. P., Sidhu, H. S., Singh, Y., Jat, H. S., Kakraliya, S. K., & Yadav, A. K. (2015). Conservation agriculture practices for enhancing productivity of cotton-wheat system. *Haryana J. Agron, 31,* 67-74.

Chen, X. Q., Smith, J. S., & Lucas, J. (1990). Microcomputer controlled arc oscillator for automated TIG welding. *Journal of Microcomputer Applications, 13,* 347-360.

Dhandha, K. H., & Badheka, V. J. (2015). Effect of activating fluxes on weld bead morphology of P91 steel bead-on-plate welds by flux assisted tungsten inert gas welding process. *Journal of Manufacturing Processes, 17,* 48-57.

Dixit, P., & Jani, S. (2020). Techniques to weld similar and dissimilar materials by ATIG welding –an overview. *Materials and Manufacturing Processes,* 1-16.

Fu, L., Yang, Y., Zhang, L., & Wu, Y. (2019). Preparation and characterization of fluoride-incorporated plasma electrolytic oxidation coatings on the AZ31 magnesium alloy. *Coatings, 9,* 826.

Fujii, H., Sato,T., Lu, S., & Nogi, K. (2008). Development of an advanced A-TIG (AA-TIG) welding method by control of marangoni convection. *Materials Science and Engineering, 495,* 296-303.

Guiqing, Z., Yingleli, R., & Yunhai, S. (2020). Research for microstructure and mechanical properties of AZ91 magnesium alloy welded joint with magnetic field and activated flux. *Materials Research Express, 7,* 056511/1-14.

Howse, D. S., & Lucas, W. (2000). Investigation into arc constriction by active fluxes for tungsten inert gas welding. *Science and Technology of Welding and Joining, 5,* 189-193.

Hui, L., & JiashengiI, Z. (2017). Study of 2219 aluminium alloy using direct current A-TIG welding. *International Journal of Modern Physics B, 31,* 1744043/1-5.

Katoh, S. (1990). Pulsed TIG welding of aluminium. *Welding International*, 4, 944-953.

Korkman, E., & Meran, C. (2020). Mechanical properties and microstructure characterization of GTAW of micro-alloyed hot rolled ferritic XPF800 steel. *Engineering Science and Technology, An International Journal,* 1-11.

Kumar, A., Chauhan, V., & Bist, S. A. (2013). Role of artificial neural network in welding technology: A survey. *International Journal of Computer Applications, 67,* 32-37.

Kumar, V., Lucas, B., Howse, D., Meltron, G., Raghunathan, S., & Vilarinho, L. (2009). Investigation of the A-TIG mechanism and productivity benefits in TIG welding. *Paper* *presented at 15th International Conference on the Joining of Materials (JOM 15) and 6th International Conference on Education in Welding (ICEW 6) Helsingor,* Denmark.

Kumar, V., Lucas, B., & Raghubathan, S. (2009). *Successful high-productivity welding with A-TIG Process.* 20th International Congress of Mechanical Engineering. Proceedings of COBEM.

Kuo, C. H., Tseng, K. H., & Chou, C. P. (2011). Effect of activated TIG flux on performance of dissimilar welds between mild steel and stainless steel. *key engineering materials, 479,* 74-80.

Leconte, S. P., Paillard, P., Chapelle, G., & Saindrenan, H. J. (2007). Effects of flux containing fluorides on TIG welding process. *Science and Technology of Welding and Joining, 1718,* 120-126.

Li, C., Shi, Y., Gu, Y. F., Fan, D., & Zu, M. (2018). Effects of different activating fluxes on the surface tension of molten metal in gas tungsten arc welding. *Journal of Manufacturing Processes, 32,* 395-402.

Li, H., & Zou, J. (2017). Study of 2219 aluminum alloy using direct current A-TIG welding. *International Journal of Modern Physics, 31,* 16-19.

Li, H., Zou, J. S. Yao, J. S., & Peng, H. P. (2017). Uniform design and optimization of active agent and technology research for A-TIG welding of 2219 aluminum alloy. *The International Journal of Advanced Manufacturing Technology,* 1-12.

Li, S. Z., Shen, J., Cao, Z. M., Wang, L. Z., & Xu, N. (2012). Effects of mix activated fluxes coating on microstructures and mechanical properties of tungsten inert gas welded AZ31 magnesium alloy joints. *Science and Technology of Welding and Joining, 17,* 467-475.

Lin, H. L., & Wu, T. M. (2012). Effects of activating flux on weld bead geometry of inconel 718 alloy TIG welds. *Materials and Manufacturing Processes, 27,* 1457-1461.

Lin, Y., & Yang, M. (2020). The effects of radiation on heat and mass transfer of magneto hydrodynamic marangoni flow in the boundary layer over a disk. *Korean Journal of Chemical Engineering, 37,* 37-45.

Liu, L., & Su, N. H. (2008). Study of flux assisted TIG welding of magnesium alloy with SiC particles in flux. *Materials Research Innovations, 12,* 47-51.

Liu, L., Zhang, Z., Song, G., & Shen, Y. (2006). Effect of cadmium chloride flux in active flux TIG welding of magnesium alloys. *Materials Transactions, 47,* 446- 449.

Maduraimuthu, V., Vasantharaja, P., Vasudevan, M. & Panigrahi, B. (2021). Microstructure and mechanical properties of 9Cr-0.5Mo 1.8W-VNb (P92) steel weld joints processed by fusion welding. *Materials Science and Engineering: A. 813, 141186,* 1-14. 10.1016/j.msea.2021.141186.

Magudeeswaran, G. & Sreehari, R. N., Sundar, L. & Harikannan, N. (2014). Optimization of process parameters of the activated tungsten inert gas welding for aspect ratio of UNS S32205 duplex stainless steel welds. *Defence Technology. 10(3),* 1-10. 10.1016/j.dt.2014.06.006.

Manivannana, S., Vairamuthu, J., Velmurugan, P., Manohar, J. N., Kannan, C. R., & Stalin, B. (2020). Electrochemical studies and corrosion resistance of activated tungsten inert gas AISI SS316L weldments studies and corrosion resistance of activated tungsten inert gas AISI SS316L weldments. *IOP Electrochemical Conference Series: Materials Science and Engineering, 988,* 012107.

Moghaddam, M. A., & Kolahan, F. (2020a). Modeling and optimization of flux assisted tungsten inert gas welding process using taguchi method and statistical analysis. *Amirkabir Journal of Mechanical Engineering, 4,* 1-9.

Moghaddam, M. A., & Kolahan, F. (2020b). Optimization of A-TIG welding process using simulated annealing algorithm. *Journal of Advanced Manufacturing Systems, 19,* 1-23.

Moghaddam, M. A., & Kolahan, F. (2021). Optimization of enhanced TIG welding process using artificial neural network and heuristic algorithms. *Research Square,* 1-19.

Mohan, P. (2014). *Study of the effects of welding parameters on TIG welding of aluminium Plate, a Master of Technology (Production Engineering)* thesis submitted to NIT, Rourkela, India.

Niagai, J. (2021). Influence of activated fluxes on the bead shape of A-TIG welds on carbon and low-alloy steels in comparison with stainless steel AISI 304L. *Metals, 11,* 1-13.

Pandya, D., Badgujar, A., & Ghetity, N. (2020). A novel perception toward welding of stainless steel by activated TIG welding: a review.

Materials and Manufacturing Processes, 36(3), 1-27.

Paspulla, A. P., Agisho, H. A., Seetharaman, S., & Vijayakumar, S. (2022). Characterization and analysis of TIG welded stainless steel 304 alloy plates using radiography and destructive testing techniques. *Materials Today: Proceedings, 51,* Part 1, 935-3.

Patel, D., & Jani, S. (2020). ATIG welding: a small step towards sustainable manufacturing. *Advances in Materials and Processing Technologies,* 1-22.

Patel, D., Jani, S., Singh, V., & Ashutosh, S. (2021). Develop a sustainable welding procedure for chromium manganese austenitic stainless steel using the ATIG process. *Engineering Research Express, 3*, 1-12.

Patel, N. P., Badheka, V. J., Vora, J. J., & Upadhyay, G. H. (2019). Effect of oxide fluxes in activated tig welding of stainless steel 316LN to low activation ferritic/martensitic steel (LAFM) dissimilar combination. *Transactions of the Indian Institute of Metals,* 1-19,

Ramkumar, K. D., Chandrasekhar, A., Singh, A. K., Ahuja, S., Agarwal, A., & Arivazhagan, N. (2015). Comparative studies on the weldability, microstructure and tensile properties of autogeneous TIG welded AISI430 ferritic stainless steel with and without flux. J*ournal of Manufacturing Processes, 20,* 54-69.

Ramkumar, K. D., Varma, J. L. N., Chaitanya, G., Logesh, S., Krishnan, V., & Arivazhagan, N. (2015). Experimental investigations on the sio_2 flux-assisted GTA welding of super-austenitic stainless steels. *The International Journal of Advanced Manufacturing Technology, 93,* 129-131.

Reddy, G. M., Gokhale, A. A., & Rao, K. P. (1998). Optimisation of pulse frequency in pulsed current gas tungsten arc welding of aluminium–lithium alloy sheets. *Materials Science and Technology, 14,* 61-66.

Roy, S., Samaddar, S., Uddin, M. N., Hoque, A., Mishra, S., & Das, S. (2017). Effect of acting flux on penetration in A-TIG welding of 316 stainless steel. *Indian Welding Journal, 50,* 72- 80.

Ruckert, G., Perry, N., & Marya, S. (2014). Enhanced weld penetrations in GTA welding with activating fluxes - case studies: plain carbon & stainless steels, titanium and aluminum. *Science Arts & Metiers (SAM), 2,* 1- 6.

Saha, S., & Das, S. (2018). Investigation on the effect of activating flux on tungsten inert gas welding of austenitic stainless steel using AC polarity. *Indian Welding Journal, 51,* 84-92.

Saha, S., & Das, S. (2019). Application of activated tungsten inert gas (A-TIG) welding towards improved weld bead morphology in stainless steel specimens. Annual Technical Volume of Production Division Board of The Institution of Engineers (India), 4, 13-23.

Saha, S., & Das, S. (2020). Effect of Polarity and Oxide Fluxes on Weld Bead Geometry in Activated Tungsten Inert Gas (A-TIG) welding. *Journal of Welding and Joining, 38,* 380-388.

Saha, S., Paul, B. C., & Das, S. (2021). Productivity improvement in butt joining of thick stainless steel plates through the usage of activated TIG welding. *SN Applied Sciences, 3*(4), 1-14. 10.1007/s42452-021-04409-7.

Sahu, N., Barik, B. K., Sahoo, S., Badjena, S. K., & Sahoo, S. K. (2021). Studies on metallurgical and corrosion characteristics of dissimilar GTAW welding of alloy 800 and SS316L using multi component activated flux. *Materials Today: Proceedings, 44,* 2533-2536.

Sándor, T., & Dobranszky, J. (2007). The Experiences of activated tungsten inert gas (ATIG) welding applied on 1.4301 type stainless steel plates. *Materials Science Forum, 537.* 63-70. 10.4028/www.scientific.net/MSF.537-538.63.

Shahroudi, F. Z., & Halvaei, A. (2019). *Effect of activating flux on the weld bead geometry andmicrostructure in TIG Welding of AISI 4140 steel.* Paper Presented on 8th International Conference on Materials Engineering and Metallurgy. 7-8th October, Teheran, Iran.

Sharma, P., & Dwivedi, D. K. (2021). Study on Flux assisted-Tungsten inert gas welding of bimetallic P92 martensitic steel-304H austenitic stainless steel using SiO_2–TiO_2 binary flux. *International Journal of Pressure Vessels and Piping, 192,* 1-13.

Shen, J., Li, S., Zhai, D., Wen, L., Liu, K., & Dai, Y. (2013). Effects of SiC on the strengthening activated tungsten inert gas (SA-TIG) welded of magnesium alloy. *Materials and Manufacturing Processes, 28,* 1240-1247.

Shen, J., Zhai, D. J., Liu, K., & Cao, Z. M. (2014). Effects of welding current on properties of A-TIG welded AZ31 magnesium alloy joints with TiO_2 coating. *Transactions of Nonferrous Metals Society of China, 24,* 2507-2515.

Silva, F. G. H., Pinho, A. P., Pereira, A. B., & Paiva, O. C. (2020). Evaluation of welded Joints in P91 steel under different heat-treatment conditions. *Metals,* 10, 1-23.

Singh, A. K., Dey, V., & Rai, R. N. (2017). Techniques to improve weld penetration in TIG welding: A review. *Materials Today: Proceedings, 4,* 1252-1259.

Singh, S. R., & Khanna, P. (2021). A-TIG (activated flux tungsten inert gas) welding: A review. *Materials Today: Proceedings, 44,* 808-820.

Song, G., Li, T., Yu, J., & Liu, L. (2018). A Review of bonding immiscible Mg/Steel dissimilar metals. *Materials (Basel), 11,* 2515/1-2.

Tanaka, M., Shimizu, T., Terasaki, T., Ushio, M., Koshiishi, F. & Yang, C. L. (2000). Effect of activating flux on arc phenomena in gas tungsten arc welding. *Science and Technology of Welding and Joining, 5,* 397-402.

Unni, A. K., & Vasudevan, M. (2020). Numerical modelling of fluid flow and weld penetration in activated TIG welding. *Materials Today: Proceedings, 27,* 2768-2773.

Varshney, D., & Kumar, K. (2021). Effects of activating flux on aluminum 6061 using TIG welding (GTAW). *AIP Conference Proceedings, 2341,* 040029, 1-5.

Vasantharaja, P., & Vasudevan, M. (2012). Studies on A-TIG welding of low activation ferritic/martensitic (LAFM) steel. *Journal of Nuclear Materials, 421,* 117-123.

Venkatesan, G., George, J., & Sawmyasri, M. (2014). Effect of ternary fluxes on depth of penetration in A-TIG welding of AISI 409 Ferritic stainless steel. *Procedia Materials Science, 5,* 2402-2410.

Vinothkumar, H., Balkrishnan, M., Gulanthaivel, K., Logeshwaran, R., & Mohanraj, R. (2020). Investigation on effects of flux assisted GTAW welding process on mechanical, metallurgical characteristics of dissimilar metals SS 304 and SS 316 L. *Materials Today: Proceedings, 33,* 3191-3196.

Vora, J., Patel, V. K., Srinivasan, S., Chaudhari, R., Pimenov, D. Y., Giasin, K., & Sharma, S. (2021). Optimization of Activated Tungsten Inert Gas Welding Process Parameters Using Heat Transfer Search Algorithm: With Experimental Validation Using Case Studies. *Metals, 11,* 1-16.

Vora, J. J., & Badheka, V. J. (2015). Experimental investigation on mechanism and weld morphology of activated tig welded bead-on-plate weldments of reduced activation ferritic/martensitic steel using oxide fluxes. *Journal of Manufacturing Processes, 20,* 224-233.

Wu, C. S., Ushio, M., & Tanaka, M. (1997). Analysis of the TIG welding arc behavior. *Computational Materials Science, 7,* 308-314.

Xu, Y. L., Dong, Z. B., Wel, Y. H., & Yang, C. L. (2007). Marangoni convection and weld shape variation in A - TIG welding process. *Theoretical and Applied Fracture Mechanics, 48,* 178-186.

Yong, F., Ding, F., & QinghuaiI, F. (2007). Study of mechanism of activating flux increasing weld penetration of AC A-TIG welding for aluminum alloy. *Frontiers of Mechanical Engineering in China, 2,* 442-447.

Zhang, R. H., Pan, J. L., & Katayama, S. (2011). The mechanism of penetration increase in A-TIG welding. *Frontiers of Materials Science, 5,* 109-118.

Zhou, M., Shen, J., Hu, D., Gao, R., & Li, S. (2017). Effects of heat treatment on the activated flux TIG-welded AZ31 magnesium alloy joints. *International Journal of Advance Manufacturing Technology, 92,* 3983-3990.

Zhou, Z., & Huang, Z. (2014). Experimental research of activating fluxes in A-TIG welding of 5052 aluminum alloy. *Advanced Materials Research.* 941-944. 2058-2061. 10.4028/www.scientific.net/AMR.941-944.2058.

Zou, Y., Rintaro, U., & Hidetoshi, F. (2014). Effect of oxygen on weld shape and crystallographic orientation of duplex stainless steel weld using advanced A-TIG (AA-TIG) welding method. *Materials Characterisation, 91,* 42-49.

Samarendra Acharya is, at present, working at Global Institute of Management & Technology, Krishnanagar, Nadia, West Bengal, India as an Assistant Professor. He is a Research Scholar working in the Department of Mechanical Engineering, Kalyani Government Engineering College, Kalyani under Maulana Abul Kalam Azad University of Technology, West Bengal. He has completed M.Tech in Mechanical Engineering (Manufacturing Technology) course from the Department of Mechanical Engineering, Dr. Sudhir Chandra Sur Degree Engineering College, Dum Dum affiliated to Maulana Abul Kalam Azad University of Technology, West Bengal achieving 2nd rank and winning silver medal in the university in the year of 2016. He has published 3 journal papers and 4 conference papers in the area of welding.
(E-mail: samarendraacharya2012@gmail.com)

Dr. Santanu Das is Professor and Former Head, Department of Mechanical Engineering, Kalyani Government Engineering College, Kalyani, West Bengal. He guided 12 Ph.D theses, 149 M.Tech theses and 104 B.Tech projects. He is guiding 05 Ph.D scholars. He has 191 publications in Journals, 37 in Book Chapters, and 112 in International and 176 in National Conferences. He was awarded 'Shiksha Ratna' in 2018 by Government of West Bengal as an Outstanding Teacher. He received Production Division Award and Second Prize of Railway Board 2019 from The Institution of Engineers (India) and one Best Paper award from Indian Institution of Industrial Engineering. He received Weldwell Speciality Award in 2021 and 2022 instituted by The Indian Institute of Welding for guiding two Best M.Tech Theses in welding. He received Welding Educationist Award 2022 by The Weld Fab Tech Times Magazine, Pune in November 2022.